UXO Discrimination:
Near Field, Heterogeneous and Multiple Objects

Kevin O'Neill
US Army Engineer Research and Development Center (ERDC) - CRREL
72 Lyme Rd, Hanover, NH 03755
603-646-4312
koneill@ERDC.usace.army.mil

Keli Sun, Fridon Shubitidze, and Irma Shamatava
Thayer School of Engineering, Dartmouth College, Hanover, NH, 03755

John Curtis and Janet Simms
ERDC – EL and GSL
Halls Ferry Rd, Vicksburg, MS

ABSTRACT

New techniques are presented for inferring the aspect ratios of representative objects, over an array of canonical shapes, using ultra-wideband electromagnetic induction (EMI). Particularly when combined with ground penetrating radar for inference of greatest object dimensions, this approach could allow estimation of overall target geometry. Analytical techniques based on simple resonating magnetic and electric dipoles are inaccurate when sensors pass close to the target, as is often the case in UXO surveying. Close proximity produces stronger excitation of only certain portions of the target, and parts of the target closest to the sensor contribute disproportionately strong signals. These near field effects are particularly important for targets that are composites of different metal types, which includes many if not most UXO. The stronger effects from different portions of a UXO threaten to make a muddle of unique signature identification, as signatures depend strongly on object orientation and standoff. We show frequency and distance dependence of these effects, and demonstrate where and how some unified signal forms and meaningful interpretation might still be achieved. A reduced source set approach is proposed for simple representation of complex object responses. This plays into the requirements for treating cases in which different objects are perceived simultaneously by the sensor, as in highly contaminated sites. For a hypothetical test case, an optimization (pattern matching) algorithm for multiple targets is demonstrated, utilizing spatial patterns of frequency response.

This work was sponsored by the CoE ERDC BT25 (Installation Restoration) research program, and by the Strategic Environmental Research and Development Program, projects 1122 and 1282

INTRODUCTION

In attempting to classify electromagnetic induction (EMI) responses from UXO and from competing clutter, we always seek some relatively simple, unifying signature phenomena. For example, we may examine the ratio of the (inferred) target responses to axial and transverse excitations, that is, when the primary (transmitted) magnetic field is aligned with or perpendicular to the target's principal axes. It is intuitively appealing that different inherent response strengths (eigenvalues) in different directions should relate to the object's overall geometrical aspect ratio, even for irregular shapes. But are the ratios of those responses unique, for a given object? How are they dependent on frequency, or distance from the object, or on what portion of the object faces the sensor? With the complexities of these questions in mind, we may seek to avoid over-simplification by declining to reduce targets and their responses to simple, fundamental features, such as unique eigenvalue ratios and geometrical aspect ratios. That is, we may simply rely on matching between observed response patterns and those catalogued for different targets, in all their complexity. However, as we shall show below, this strategy is vulnerable to the same complications, namely, lack of a uniquely identifiable signatures for a given object, applicable over a wide range of circumstances.

In what follows we pursue these matters by examining the linkage between inevitable near field and target heterogeneity effects. Strategies are proposed by which meaningful information about fundamental geometry of heterogeneous targets might still be extracted, by using either high frequencies or early time response; or by examining shifts in eigenvalue ratios over the entire EMI ultra-wideband. When problematical signal heterogeneity results from the spatial overlap of responses from different targets, it may still be possible to infer some fundamental features of each contributing item. We demonstrate an approach using non-linear least squares optimization to extract the eigenvalues of the individual contributing targets in such a case, by examining the pattern of frequency response over space for a hypothetical multi-object configuration. As a tool for inversion and classification processing of both single and multiple objects, we propose a target representation system based on a reduced source set. The key to application lies in decomposing an arbitrary primary field, for an arbitrary target disposition, using scalable input modes.

RESULTS

Heterogeneity Effects

Figure 1 shows a 120 mm HEAT round consisting of four sections, altogether about 80 cm long, consisting of 1) magnetic (steel), 2) non-magnetic (titanium?), 3) magnetic steel, and 4) probably aluminum. The plots show single-frequency GEM-3 responses from horizontal scans along its length at elevations of 16, 26, and 36 cm. At low but not at high frequency, distinct sections cause variation of response along the scans, when the sensor passes close to the target. As the sensor is raised, the low frequency pattern (left) still contains some influence of the disparate sections. However, at the highest elevation all sections participate simultaneously, and a smoother, almost symmetrical spatial pattern emerges, more in line with the variation in geometry along the scan length. How do we know that this low frequency variation along the length is associated with different materials, as opposed to different geometrical features? When the sensor passes close to the object, the low frequency response changes sign, depending on which section it is passing, which shows changing proximity to magnetic/ non-magnetic materials. Beyond this, the contrast to high frequency responses is suggestive (right plot, Figure 1). At 20 kHz, the signals barely penetrate the metal and thus are relatively insensitive to material type. Even for passes quite close to the object, the response is more or less symmetric about the center of the target, as is its geometry. That is, at high frequencies the response derives from surface currents, the patterns of which depend only on object geometry. In the high frequency case we see a smooth, symmetrical spatial pattern already at an elevation of 36 cm, which is only approximately half the object's length. In sum, it is erroneous to speak of "the" transverse frequency response for this UXO. It depends on what frequencies we

work with, and how close we are to the object and what its various distinct sections consist of. If we want to seek out evidence of its heterogeneity, we must pass close and examine low frequency content. If we seek evidence of its geometry, we should examine the higher frequencies. We will still see changes in spatial pattern with elevation at the high end of the spectrum, but these will not be significantly affected by material type. These considerations come to the fore as we attempt to use relations between axial and transverse responses as a basis for target classification.

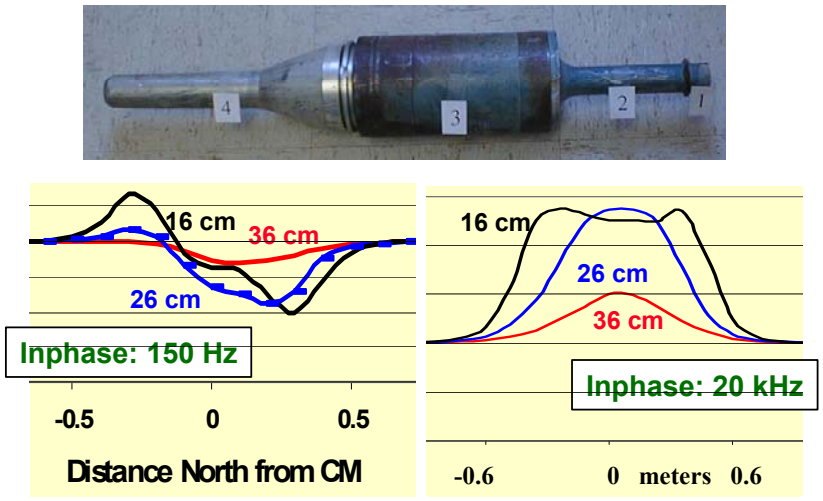

Figure 1.

120 mm HEAT round (top), consisting of four sections made of different materials. Horizontal scans along the object with a GEM-3, at the indicated elevations, produce different patterns of response at low frequency (left) and high frequency (right).

We have seen even stronger evidence of target heterogeneity when a composite object is oriented vertically, i.e. with the primary field oriented along target axis. In this case the problem may be even more challenging, if our objective is to elevate the sensor to a point where a single axial response emerges, whether the target is nose up or tail up. Specifically, two questions emerge at the outset: Whichever end of the target is facing up (towards the sensor), can we elevate the sensor to a point where a stable pattern emerges, i.e. one not affected by further changes in elevation? Will this pattern depend on which end is up, or will there be a single axial pattern for the target in question? We explored these questions by constructing a test target consisting of steel and aluminum sections, each about 3.8 by 7.6 cm, with threaded ends so that they screw together. When screwed together, the total length of the composite cylinder is about 14 cm, because of the overlap (see schematic illustration, top right in Figure 2). The intent of this fabrication is to mimic the division of materials and kind of connection between the nose and tail section of a UXO. Figure 2 (top) shows measurements obtained with a GEM-3 UWB EMI sensor, with 40 cm diameter head, operating between about 30 Hz and 50 kHz. All results in the figure are arbitrarily normalized. When the sensor is about one target length above the center of the composite cylinder, distinctly different patterns emerge depending on which material is up. In the plot on the upper left, with the steel up, the inphase and quadrature component curves cross far out in the tail of the quadrature curve, a characteristic of responses from axially oriented, elongated magnetic bodies. The pattern on the top right fails to show this feature. At the same time, the latter strongly resembles patterns we have seen from compact homogenous ferrous objects (e.g. spheres or very short cylinders), or from elongated homogeneous ferrous objects oriented *transverse* to the primary field. Thus the composite composition, in axial orientation with aluminum up, "mimics" the response of other geometries and other materials.

Also shown in the top two plots of Figure 2 are continuous curves from numerical solutions for these cases, obtained via the Method of Auxiliary Sources [1,2], including detailed representation of the object composition and of the primary field. Clearly agreement is very good, and we use the numerical model to explore effects of changing the sensor elevation. On the bottom left in Figure 2 we see computed frequency responses for the two axial orientations, obtained when the sensor is effectively at an infinite distance from the object. Gratifyingly, the patterns have converged to a single shape, resembling, as it happens, the response of an elongated magnetic object. The jury is still out on how general this result is: Here, when the sensor is far enough away, the steel portion appears ultimately to dominate the shape of the response (at

least, the relation between the components), whether that section is facing up or down. Questions remain as to whether one section of the object would "shadow" another if it were broader, a phenomenon suggested in some of our other modeling exercises. Be that as it may, the plot on the lower right of Figure 2 serves as something of an unpleasant reality check. There the simulation results show what would be obtained if the

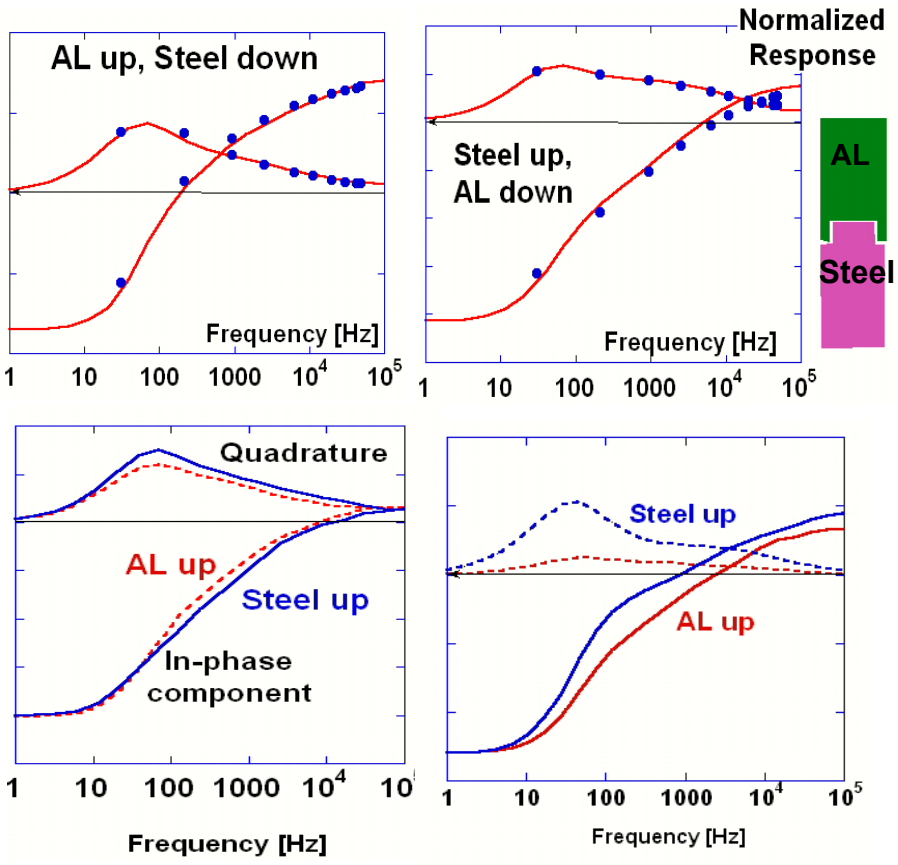

Figure 2. Top: Responses from flipped vertical orientations of a composite steel-aluminum cylinder (far right) show marked difference, in both measurement (points) and simulation (curves), when the sensor is about one cylinder length away.

Bottom: Simulations of response from an "infinite" distance (left) show that the patterns for the two vertical orientations converge at "infinity," but are still quite different (right) when the sensor is 2 m away. All responses are arbitrarily normalized.

GEM-3 were raised to 2 m above the target, and we see that the two patterns have still not converged. Further elevation of the sensor up to (an especially unrealistic) 5 m does not help appreciably. Most important (see below): While the simulation can "see" this small target at elevations like 2 to 5 m, in measurement reality we could not distinguish any meaningful signals at these distances. That is, it is not possible to move the sensor far enough away to get a single pattern, independent of which end is up. Further deflating is the fact that it will not help if we restrict ourselves to larger objects which produce stronger signals. "Infinity" is much further away for larger objects, and the stronger response by larger targets cannot compensate for the severe falloff in the fields with distance.

As a last note on vertical orientations, we pursue the suggestions in the discussion of Figure 1, to the effect that higher frequency responses show less evidence of material heterogeneity and are more simply reflective of the target geometry. Figure 3 shows time domain measurements obtained with an EM-61, for the HEAT round (Figure 1) in the alternative vertical orientations. Proportionally greater difference occurs in late time when signals penetrate the target, corresponding to the lower frequency response in the frequency domain. In very early time (corresponding to high frequencies), the flipped orientations produce very similar results, on log scale. This supports the notion that high frequency/ early time measurements might be pursued to focus on geometry, without the encumbrance of material type effects. The question remains whether enough information is present in the high frequency/early time realm for us to succeed in discrimination/ classification/ inversion.

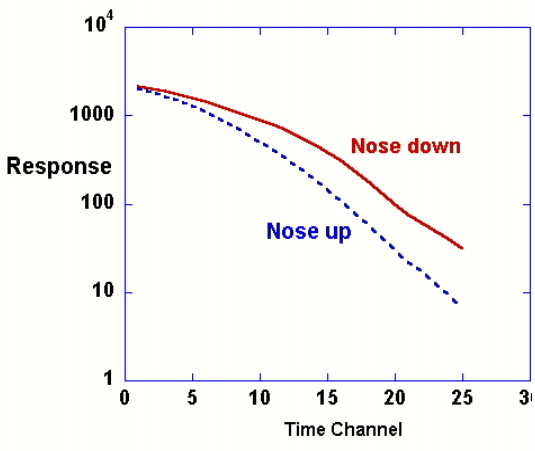

Figure 3. Time domain measurements on the HEAT round, in flipped vertical orientations, about 12 cm from the sensor head.

High Frequencies and Aspect Ratio

Pursuing the possibilities of high frequency discrimination, we consider in Figure 4 the results of rigorous numerical simulations [3,4]. Here we assume that the sensor operates at a high enough frequency to estimate the asymptotic high frequency response limit, where the target behaves as a perfect reflector. Under these conditions the primary field does not penetrate the object at all, and response is insensitive to metal type. Various geometries were investigated in that both sharp-edged and smooth shapes (cylinders and spheroids) were treated, as were elongated and flattened bodies (oblate spheroids). The figure shows the magnitude of the ratio of the transverse to axial response, in the far field, as a function of target aspect ratio, defined as length divided by diameter. While there is some difference between the curves, possibly because cylinders and the spheroids have different volumes at the same nominal aspect ratio, the pattern is clear: The ratio of the EMI responses along primary axes is directly related to the geometrical aspect ratio, such that one could in principle infer the latter from the former... at least in an ideal world. The problem lies not so much in the fact that the curves flatten out for larger aspect ratios, if our objective is simply to infer whether the object is elongated beyond a certain point or not. It is rather the small dynamic range of the parameter to be measured, i.e. of the ratio in response magnitudes. In the field, one would have to infer the responses along principal axes by moving the sensor about and indirectly calculating what the eigenvalues of the inherent response function are. However, especially when the target is shallow, small movements of the sensor can cause very large variations of the magnitude in response. The uncertainty introduced by variations in magnitude from movement of the sensor might well swamp the smaller variations in the parameter we seek. To be researched, therefore: With a sufficient sampling of response over a spatial volume around and above the target, when might it still be possible to infer the high frequency eigenvalue ratio with enough clarity to make basic shape classifications?

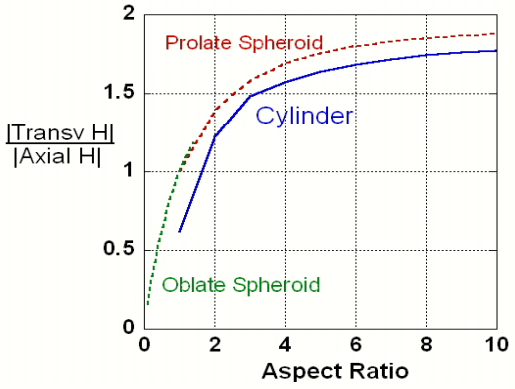

Figure 3. The ratio of transverse to axial response for cylinders and spheroids (far field) vs aspect ratio (L/D) of the target, at the EMI high frequency response limit.

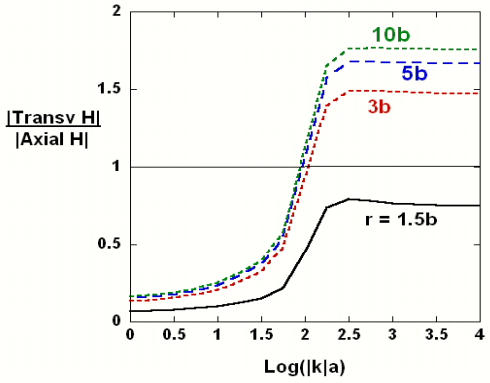

Figure 5. Computed ratio of transverse to axial response of homogeneous steel prolate spheroid observed at different distances r from target center. |ka| = induction number ~ dimensionless frequency.

Broadband Eigenvalue Ratio Patterns

Here we investigate the possibilities that may lie in retaining the concept of correlating eigenvalue ratios with aspect ratio, but returning to the use of broadband patterns. At the end of the EMI spectrum for which the results in Figure 4 apply, the transverse response is larger than the axial response, for an elongated object. This is not the case over most of the EMI spectrum. **Error! Reference source not found.** shows the eigenvalue ratio over the entire EMI spectrum, calculated numerically for a hypothetical steel prolate spheroid. The small semi-axis length is a, and long semi-axis b = 25 cm; b/a = 5, $\mu = 50\,\mu_o$. In terms of the object length $2b$, the observation distance r (from the center of the object) is $(r\text{-}b)/2b$ target lengths from the tip of the target, when it is vertically oriented. Thus, in the vertical orientation, the point $r = 1.5b$ is only one quarter object length from the end, and $r = 3b$ is only a about one object length from the end. As long as the observation point is at least one object length from its surface, we see a very distinctive pattern in the eigenvalue ratio, as a function of frequency. In particular, it reverses in the sense that it shifts from a value less than one at low frequency to a value greater than one at higher frequency. Even though the very close observation point ($1.5b$) does not produce a shift that crosses the level of unity, we still do see the same kind of characteristic S-shaped curve as at the greater observation distances. While many factors in measurement and processing might introduce some uncertainty into the eigenvalue ratio we obtain from actual data, hopefully at least this underlying broadband pattern is robust enough to be visible nonetheless. We note that for flattened objects, comparable plots of the eigenvalue ratio (not shown) display the opposite shift, from values larger than one at low frequency to magnitudes smaller than unity at high frequency.

Previously we discussed the effects of material heterogeneity on uniqueness of response from targets in different orientations. Returning to our fabricated composite test cylinder (Figure 2) we examine the eigenvalue ratio over a wide band (Figure 6). With the steel portion pointing towards the sensor (axial case), we see the same transition in ratio of transverse to axial response as for the homogeneous ferrous spheroid, particularly when the observation point is at least one object length away from the cylinder ends. However, Figure 7 shows the same experiment repeated with the aluminum end facing the sensor. Here we fail to see the previously observed pattern. Significantly, measurements were terminated in both orientations when the the sensor was elevated to the point where signals were too faint to produce meaningful data. The degeneration of signal to noise with increased standoff may account for the spread of the curves as they presumably aproach a limiting form at greater distances. In any case, while the curves cluster within a discernible envelope as elevation is increased, we do not reach clear asymptotic limits at either end of the spectrum in Figure 7. There is a persistent, local low frequency peak and the ratio never surpasses one. The evidently stronger influence of the aluminum section in this case has altered the simpler response shapes seen in Figures 5 and 6.

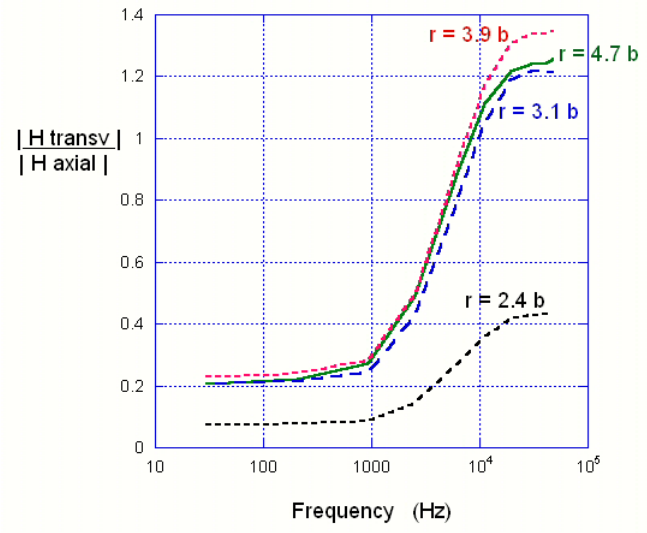

Figure 6.
Magnitude of transverse response to axial response as a function of frequency, for composite cylinder, measured at different distances r from its center .

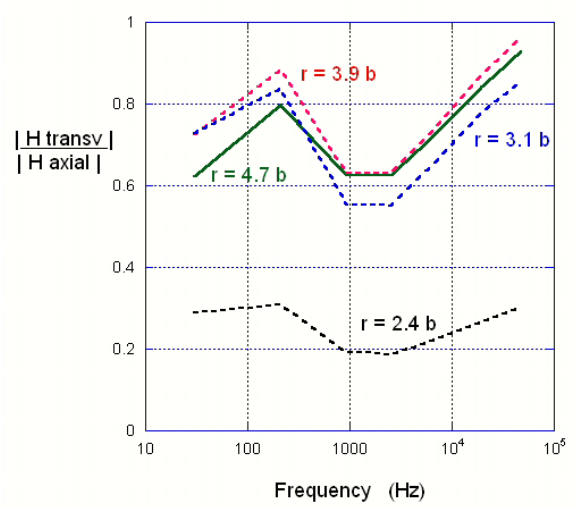

Figure 7.
Measured ratio of transverse to axial response for the same case as in Figure 6, but with the aluminum portion facing the sensor, in axial orientation, with sensor elevations indicated.

An elongated non-magnetic metallic target will generally show an eigenvalue ratio of approximately one, across the entire band. This contrasting scattering behavior, relative to the steel's, generates the more complicated picture of Figure 7. Overall, these results suggest that we might still apply a system of aspect ratio inference based on the reversal of the ratio of principal responses if the steel component dominates. With the aluminum end up, we are unlikely to be able to measure the responses from a sufficient distance so that near field effects emphasizing the aluminum portion fade. While it fails to conform to the pleasingly simple pattern in Figures 5 and 6, the pattern in Figure 7 is nonetheless distinctive. In the last section below we outline some of the analytical measures we are investigating to address these issues.

Treatment of Multiple Objects

Beyond target heterogeneity, heterogeneity of environmental conditions also contributes to the difficulty of applying inversion or classification schemes based on scattering features of simple, single objects. Here we show some preliminary results of an approach for distinguishing the characteristics of contributing objects when their sensor responses overlap spatially. In its simplest version, the system employs an idealization used elsewhere [e.g. 5], wherein an object's response is in terms of triaxial magnetic dipoles. Diagonalization of the target's magnetic polarizability tensor identifies its eigenvalues, i.e. its intrinsic magnetic dipole strengths in each principal direction, in response to unit stimulus in that direction. To incorporate this in a processing system for multiple targets, the distribution of frequency response across the space above the two targets is obtained, with both targets present simultaneously. Then we use a non-linear least squares optimization algorithm to obtain a best fit to this data, produced by different possible selections of each target's eigenvalues. That is, we attempt to infer the characteristics of each from their superposed responses. For a hypothetical case we first obtain rigorous responses for two example ferrous objects, a sphere with 5 cm radius and an ellipsoid with semi-major axis lengths of 2.9 cm, 8.7 cm, and 15 cm. Assuming that the objects are buried 0.75m deep and 0.75 m apart, we use the TSA formulation [3,4] to predict the response pattern over space produced by the two together, assuming negligible interaction but including all effects of the near field and finite geometry. The total pattern in Figure 8 shows how the responses from the two objects overlap spatially, under the idealized excitation of unit primary field strength in both horizontal and vertical directions. The optimization algorithm indeed extracted equal eigenvalues for all (any) three principal directions for the sphere. Results for the ellipse are shown in Figure 9. We do indeed see very good agreement between the "real" (numerically obtained) eigenvalues, and those inferred via the processing of the combined data with the dipole models.

In ongoing work, we investigate the utility and limitations of this kind of processing, in both simulation and measurement, varying the spacing of the targets and their types as well as the survey

strategy. From the other material presented in this paper, we know that a dipole model for each contributing target is itself quite a limiting idealization. The next section outlines a higher fidelity method for respresenting the responses of complex targets, while retaining sufficient simplicity to allow the many repeated computations required in typical inversion processing.

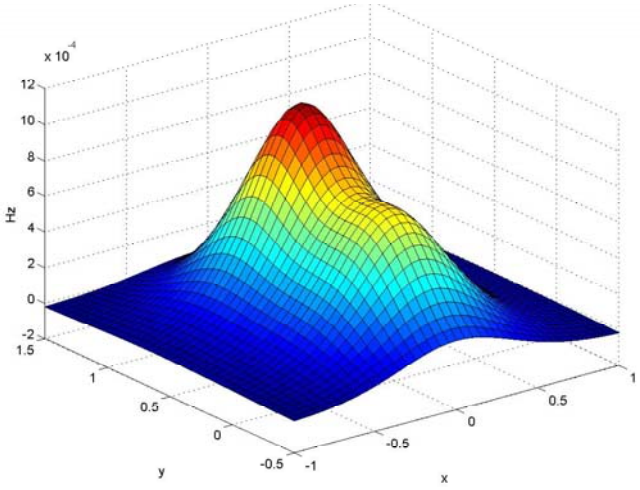

Figure 8. Signal magnitude pattern over space produced by the buried sphere and ellipsoid together, as determined using the TSA program.

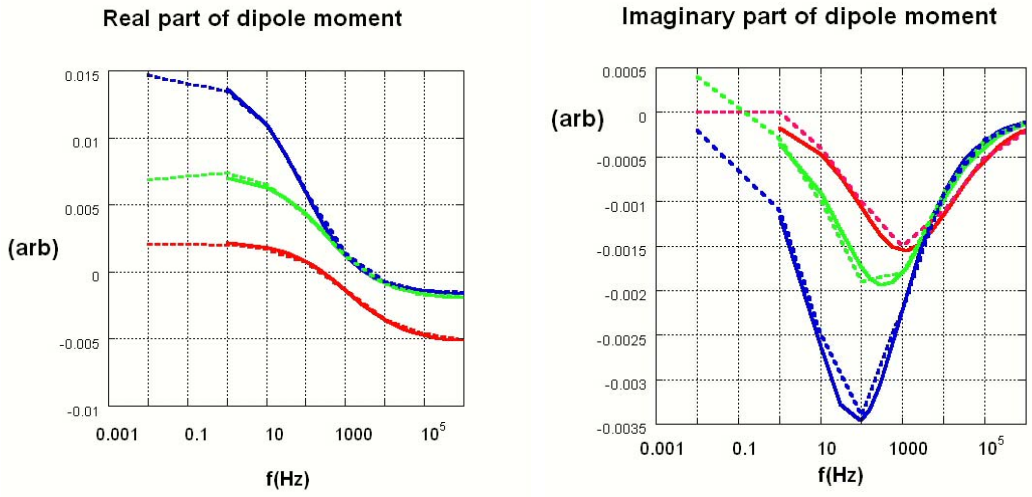

Figure 9 Eigenvalues of magnetic polarizability tensor for the ellipse, along three principal axes, determined by detailed numerical modeling of the object alone (solid lines), and by inference via best fits to point dipole models using combined sphere and ellipsoid response data (dashed).

Object Representation for Inversion and Classification Processing

In our modeling of UXO and other representative metal targets, we have resorted to detailed, rigorous numerical models. These have succeeded in representing the responses of many types of targets quite well, and have served as a valuable means of obtaining insights into fundamental scattering behavior in the EMI band. At the same time, because they may require signficant computational resources for each run, these

models are often not well suited for some calculations typically required for inversion and classification processing. In such processing, we may need to examine many possible solutions very quickly to obtain a best fit between observation and various theoretical possibilities. To some extent, this need can be met by new analytical solutions that have been developed for homogeneous objects with basic non-spherical shapes [6,7]. But the material above illustrates that we must be able to represent geometrically complex, materially heterogeneous objects as well.

Some of our numerical modeling works by expressing the magnetic fields in terms of a superposition of fields from a finite number of simple sources distributed around and within the object [1,2]. While we typically use many such auxiliary sources to obtain an accurate, rigorous solution, it should be possible to represent the scattered fields using a very reduced set of sources, at least when the observation point is some modest distance from the target surface. To this end, consider the construction in Figure 10. The hpothetical target on the right may in fact be quite heterogeneous, both materially and geometrically. For any given input (primary) field, we can solve rigorously for the response perceived at any given observation point or plane. Alternatively, we may obtain this information from measured data. The problem lies in using a this sort of data from a limited number of observations to predict the target response from *any* input, as perceived at *any* observation point. The latter task is not so difficult if we construct the response based on some well defined set of reaction sources induced in the target. Once we know those for any given input, we can examine the corresponding output anywhere, using standard relations. We have seen above that, in some limited cases, a very simple source distribution suffices, e.g. point magnetic dipole at the object's center, with observation point relatively far away. But especially for hetergeneous objects we will need to construct the scattered field from more sources. Thus we hypothesize a system with an expanded, but still quite limited number of sources distributed over the target volume, from which more complicated scattering behavior can be represented quickly and easily (e.g.Figure 10). Because the magneto-quasistatic field exterior to the target satisfies the Laplace equation, we work in terms of fictitious magnetic charges. With high magnitudes clustered near the object center, these can approximate a point magnetic dipole; clustered at the ends they can represent a single dipole of finite length; or their magnitudes can be distributed more arbitrarily to produce more complicated response fields.

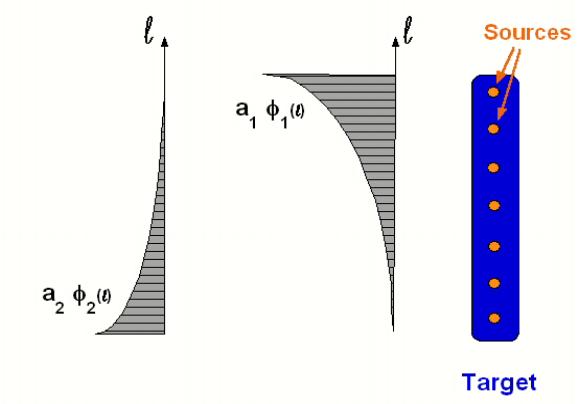

Figure 10.

Target containing distribution of point sources of arbitrary magnitude, with two differently scaled input mode shapes illustrated.

The key to making use of this approach lies in decomposing the primary excitation field into *scalable* modes. In radar problems, for example, we can solve for the target's response to unit magnitude plane waves propagating in a variety of directions. Recording the solution means retaining the source strengths (electric and magnetic surface current values) produced by each of these representative inputs. When the target is located anywhere near a particular radar antenna, the incident beam pattern striking the object can be approximated by a superposition of plane waves. In turn, the scattered field can be constructed from a corresponding superposition of the scattered fields associated with each of those "inputs." In the EMI realm there are no plane waves; in fact, there are no waves. Thus we must resort to some other basis for representing inputs and their induced source distributions within the target. This can be done using scalable mode shapes, e.g. polynomials, as illustrated schematically in Figure . Typically we are able to produce

rather accurate quantitative representations of the primary fields from common EMI survey systems. To proceed, we first obtain the target response to each i^{th} input mode shape $\phi_i(\ell)$, where ℓ is distance along the target's axis. These are easily stored. For each prospective target location and orientation, we decompose each of the vector components of the primary field into a linear combination of these $\phi_i(\ell)$. It is likely that no higher than cubic forms would be required, if that. Thus the primary field would be represented as $\mathbf{H}^{PR} = \sum_{i=1}^{N} \mathbf{a}_i \phi_i(\ell)$, where the $\mathbf{a}_i$ are scaling constants. The corresponding scattered field can be obtained quickly by scaling the source strengths associated with each $\phi_i(\ell)$ by the same set of $\mathbf{a}_i$. Testing of this concept is underway.

CONCLUDING DISCUSSION

In the EMI responses of heterogeneous objects, we have seen distinct effects in both horizontal and vertical orientations. In the horizontal case, proximity to different materials is evident as a survey scan passes near each portion of the target. This occurs at low frequencies when the signals penetrate the object significantly and thereby react to material type. While these horizontal, low frequency response patterns coalesce to a single shape as one elevates the sensor, the same cannot be said when the object is vertically oriented, i.e. with the primary field aligned more or less with the axis of the object. The investigations reported here suggest that, for realistic UXO/clutter sizes, one can never move the sensor far enough away to produce a single, spatially stable pattern over the EMI band. The exception to this may lie in the high frequency or early time realm, where material type is not important. We show that, in principle, the high frequency eigenvalue ratio could provide a material-independent estimation of aspect ratio. Questions arise, however, as to whether the dynamic range of the high frequency eigenvalue ratio is sufficient to be heard above the noise. Alternatively, shifts in the pattern of eigenvalue ratio over the whole EMI ultra-wideband offer some hope for inferring aspect ratio, even for composite targets, at least when steel dominates the response. Further analysis is required for cases where prominence of non-magnetic components complicates the picture. Signal heterogeneity may result from multiple targets perceived simultaneously. In a hypothetical case, we apply a non-linear least squares optimization algorithm which succeeds in extracting information about each contributing object from the spatial distribution of their combined frequency response. For application in more realistic scenarios, as well as in single-target cases with composite objects, we propose a reduced source set formulation. This system should be capable of allowing rapid examination of realistically complex responses from prospective targets, in the course of inversion and classification processing.

REFERENCES

1. F. Shubitidze, K. O'Neill, S. Haider, K. Sun, and K.D. Paulsen, "Application of the method of auxiliary sources to the wideband electromagnetic induction problem," IEEE-Trans. Geosci. Remote Sensing, vol 40, No 4, pp.928-942, 2002.
2. F. Shubitidze, K.O'Neill, K.Sun and K.D. Paulsen, "Investigation of broadband electromagnetic induction scattering by highly conductive, permeable, arbitrarily shaped 3-D objects," submitted for publication, 2002.
3. K. Sun, K. O'Neill, S.A. Haider, and K.D. Paulsen, "Simulation of electromagnetic induction scattering from targets with negligible to moderate penetration by primary fields," IEEE Trans. Geosci. Remote Sensing, vol 40, No 4, pp.910-927, 2002.
4. K. Sun , K. O'Neill, F. Shubitidze, I. Shamatava and K.D. Paulsen, "Theoretical analysis of TSA formulation and its domain of validity," submitted for publication, 2002.
5. L. Carin, H. Yu, Y. Dalichaouch, A.R. Perry, P.V. Czipott, and C.E. Baum, "On the wideband EMI response of a rotationally symmetric permeable and conducting target," IEEE Trans. Geosci. Remote Sensing, vol. 39, no 6, pp. 1206-1213, 2001.
6. H. Braunisch, C.O. Ao, K. O'Neill, and J.A. Kong, "Magneto-quasistatic response of conducting and permeable prolate spheroid under axial excitation," IEEE Trans. Geosci. Remote Sensing, vol. 39, pp.2689-2701, 2001.
7. C.O Ao, H. Braunisch, K. O'Neill, and J.A. Kong, Quasi-magnetostatic solution for a conducting and permeable spheroid with arbitrary excitation, IEEE Trans. Geosci. Remote Sensing, Vol 40, no 4, pp.887-897, 2002.